ELSEVIER

Thin Solid Films 294 (1997) 112–117

thin solid films

Optical and electrical properties of $Si_{1-x-y}Ge_xC_y$ thin films and devices

A.St. Amour, L.D. Lanzerotti, C.L. Chang, J.C. Sturm

Department of Electrical Engineering, Princeton University, Princeton, NJ 08544, USA

Abstract

$Si_{1-x-y}Ge_xC_y$ thin films grown by low temperature chemical vapor deposition containing up to 1.2% substitutional C were incorporated into microelectronic devices. The chief aims are to demonstrate that the material is of suitable quality for device applications and to use the electrical and optical characteristics of the devices to study the material. Three sets of devices containing epitaxial $Si_{1-x-y}Ge_xC_y$ layers were fabricated and characterized. The temperature dependence of the collector current in $Si_{1-x-y}Ge_xC_y$ base heterojunction bipolar transistors indicated that the band gap of $Si_{1-x-y}Ge_xC_y$ increases +26 meV $\%C^{-1}$. Capacitance measurements on p^+-$Si_{1-x-y}Ge_xC_y$/p^--Si heterojunction internal photoemission structures indicated that the increase in band gap in the $Si_{1-x-y}Ge_xC_y$ is due primarily to downward movement of the valence band. Finally, $Si_{1-x-y}Ge_xC_y$ p–i–n diodes showed no degradation in reverse bias leakage compared with C-free devices for $y < 0.01$. However, the diodes did exhibit excess sub-band gap absorption which increased with [C].

Keywords: Optical properties; Electrical properties; Silicon; Germanium

1. Introduction

The addition of small amounts of carbon (approximately 1%–2%) to $Si_{1-x}Ge_x$ has been shown to reduce the compressive misfit strain in thin films grown pseudomorphically on Si(001) substrates [1,2]. Previous photoluminescence measurements showed that the addition of 1% carbon to $Si_{1-x}Ge_x$ increased the band gap by 21–23 meV [3,4]. The initial incorporation of substitutional carbon into pseudomorphic $Si_{1-x}Ge_x$ is expected to have two separate effects on the band gap:

$$\Delta E_{G,total} = \Delta E_{G,strain} + \Delta E_{G,intrinsic} \quad (1)$$

First, by compensating the misfit strain due to the Ge, the C will tend to increase the band gap of the material $\Delta E_{G,strain}$. Additionally, because the C atoms themselves induce local fluctuations in the crystal potential, they will have an intrinsic effect on the band gap of relaxed $Si_{1-x-y}Ge_xC_y$ $\Delta E_{G,intrinsic}$. By subtracting the first effect (that of the strain reduction) from the measured $\Delta E_{G,total}$, $\Delta E_{G,intrinsic}$ was found to be −20 meV $\%C^{-1}$ [4]. That is, the initial incorporation of substitutional C into relaxed $Si_{1-x-y}Ge_xC_y$ decreases the band gap, despite the large band gaps of diamond and SiC. The work of Brunner et al. [5] showed that $\Delta E_{G,intrinsic}$ for $Si_{1-y}C_y$ was also −20 meV $\%C^{-1}$, indicating that the intrinsic effect of C on the band gap is similar in $Si_{1-x}Ge_x$ and in Si.

In previous papers, we and others have reported evidence that, for a given band gap, $Si_{1-x-y}Ge_xC_y$ has less misfit strain and a greater critical thickness than does C-free $Si_{1-x}Ge_x$ [3,4]. That is, reducing the strain in $Si_{1-x}Ge_x$ by adding C increases the band gap less than does reducing the strain by merely removing Ge. Assuming that one C atom compensates the misfit strain due to 8.3 Ge atoms and that a few per cent C does not alter significantly the elastic properties of $Si_{1-x-y}Ge_xC_y$, we have computed the expected equilibrium critical thickness h_{crit} [6] for $Si_{1-x-y}Ge_xC_y$ alloys. In Fig. 1, we have plotted h_{crit} as a function of band gap offset to Si. For large ΔE_G (greater than 250 meV), h_{crit} is increased only by a factor of approximately 0.4 $\%C^{-1}$. However, for a smaller, but still useful, $\Delta E_G = 100$ meV, h_{crit} is enhanced by

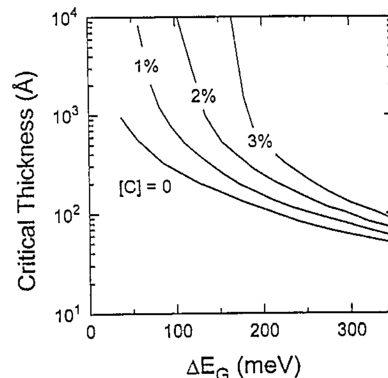

Fig. 1. Comparison of the critical thickness/band gap trade-off for $Si_{1-x}Ge_x$ and for $Si_{1-x}Ge_xC_y$. The critical thickness is from the Matthews–Blakeslee equilibrium model [6], assuming that the elastic properties of $Si_{1-x-y}Ge_xC_y$ are the same as those of $Si_{1-x}Ge_x$.

0040-6090/97/$17.00 © 1997 Published by Elsevier Science S.A.
PII S0040-6090(96)09212-7

more than a factor of two when only 1% C is added and is greater than 1 μm for $y = 0.02$. Based on this, pseudomorphic $Si_{1-x-y}Ge_xC_y$ appears promising for extending the application of Si-based heterostructures to devices requiring thicker films.

In this paper, we discuss the fabrication of three sets of electrical devices containing strained $Si_{1-x-y}Ge_xC_y$ epitaxial thin films. The emphasis is on demonstrating that $Si_{1-x-y}Ge_xC_y$ can be formed with sufficient quality to be used in minority carrier devices, and on using the devices to measure the band structure of the material. Temperature-dependent collector current measurements on $Si_{1-x-y}Ge_xC_y$ base heterojunction bipolar transistors (HBTs) [7] indicated that the band gap increased 26 meV $\%C^{-1}$, in close agreement with the optical measurements. Capacitance measurements on p^+-$Si_{1-x-y}Ge_xC_y$/p^--Si heterojunction internal photo-emission (HIP) structures indicated that most of the increase in band gap is due to downward movement of the valence band. $Si_{1-x-y}Ge_xC_y$ p–i–n diodes demonstrated no degradation in reverse bias *I–V* behavior for $y < 1\%$ C, but did show evidence of increased defect-related sub-band gap absorption compared with a C-free device.

All of the structures used in this work were grown by rapid thermal chemical vapor deposition. The $Si_{1-x-y}Ge_xC_y$ layers were grown at a pressure of 6 Torr and at temperatures between 550 and 625 °C, using dichlorosilane, germane, and methylsilane as precursors [8]. The device structures were all in situ doped with diborane and phosphine. The reported C concentrations were determined by X-ray diffraction (XRD). Assuming that the Ge contents were unchanged by the addition of methylsilane at constant germane flow and that one C atom compensated the strain due to 8.3 Ge atoms, the shift in the $Si_{1-x-y}Ge_xC_y$ (400) XRD peak towards the Si substrate peak was used to quantify the C content.

2. $Si_{1-x-y}Ge_xC_y$ heterojunction bipolar transistors

2.1. Fabrication

Heterojunction bipolar transistors (HBTs) with $Si_{1-x-y}Ge_xC_y$ bases and Si emitters and collectors were fabricated from an in situ doped epilayer structure. Two sets of transistors were fabricated: in one set the $Si_{1-x-y}Ge_xC_y$ bases were grown at 550 °C, in the other the bases were grown at 625 °C. For all devices at both temperatures, all precursor gas flows were kept constant, except for methylsilane which was varied to adjust the C content of the bases.

For the devices with bases grown at 550 °C, the epi-stack consisted of a 5 μm n^+ buffer grown at 1000 °C on 20 Ω cm, 100 mm Si(001) substrates. This n^+ buffer was followed by a 6000 Å n^- collector doped with P between 10^{16} and 10^{17} cm^{-3}. The approximately 500 Å $Si_{1-x-y}Ge_xC_y$ bases were doped with 7×10^{19} cm^{-3} B and had approximately 70 Å undoped $Si_{1-x-y}Ge_xC_y$ spacer layers on either side. The 600 Å, 8×10^{18} cm^{-3} P doped emitter was grown at 700 °C and was followed by an 800 Å, 2×10^{19} cm^{-3} doped emitter contact layer. The structures with their bases grown at 625 °C were similar, but with a base doping approximately 10× lower and a lightly doped collector of only 2000 Å.

Large-area devices were fabricated using a simple double mesa process. The base was revealed by a selective wet etch which defined the emitter-base junction area, while the collector-base junction was defined by dry etching a larger mesa around the emitter-base mesa. This process leaves the device perimeter unpassivated, leading to large, non-ideal base currents. It is, however, adequate for measuring the ideal collector currents needed to measure changes in the band gap of the base.

2.2. Band gap measurement

It is well known that the difference in band gap between the base regions of two HBTs may be extracted from the dependence of their collector currents on temperature [9]. The ratio of the collector current in HBTs with different base composition is

$$\frac{I_{C1}}{I_{C2}} = \frac{N_{G2}(N_c N_v)_1 D_{n1}}{N_{G1}(N_c N_v)_2 D_{n2}} \exp(\Delta E_A / kT) \quad (2)$$

where N_{Gi} is the base Gummel number, $(N_c N_v)$ is the product of the effective conduction and valance band densities of states, and D_{ni} is the electron diffusion coefficient. If there are no parasitic barriers in the conduction band, such as those resulting from conduction band offsets ΔE_c in abrupt junction devices without undoped spacer layers [10], or those resulting from base out-diffusion into the emitter and collector regions [11,12], then the activation energy E_A is the change in band gap between the two base materials ΔE_G. This no-barrier assumption is justified in our case since $\Delta E_c \sim 0$ in the strained $Si_{1-x}Ge_x$/Si system [13] and because the undoped spacers in our devices would prevent any barrier formation caused by boron diffusion or by any small ΔE_c induced by carbon. The high early voltages of the devices and identical collector currents in forward and reverse mode support this assumption.

Forward active Gummel plots were measured from 180 to 360 K. Fig. 2 shows the ratio $I_{C,SiGeC}/I_{C,SiGe}$ at $V_{BE} = 0.55$ V

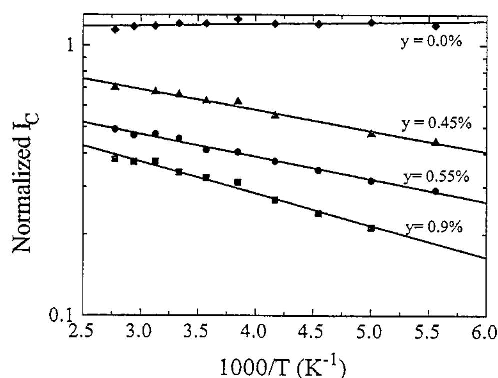

Fig. 2. Normalized collector current ($I_{C,SiGeC}/I_{C,SiGe}$) as a function of inverse temperature for the 625 °C devices with $x = 0.2$ and $0 \leq y \leq 0.9$.

as a function of inverse temperature. Assuming a similar temperature dependence of the electron diffusion coefficient and density of states between the two samples, ΔE_G was extracted from the slope of the data. As seen in the figure, carbon incorporation clearly led to an increased band gap. Fig. 3 shows the change in band gap as a function of C concentration for devices with $x=0.2$ (625 °C) and $x=0.25$ (550 °C). Note that there is no substantial difference in the change in band gap between the 550 and 625 °C films. The best straight-line fit gives $\Delta E_G/\Delta y = 26$ meV %C^{-1}.

As mentioned above, the effect of C on the band gap of pseudomorphically strained $Si_{1-x-y}Ge_xC_y$ alloys has been measured previously by photoluminescence (PL), and the measured changes in band gap were 21–24 meV %C^{-1} [3,4]. That our transport measurements and the PL measurements yield a similar result is significant. Severe local lattice distortion is known to occur around the C atoms in $Si_{1-x-y}Ge_xC_y$ films [14], and this relaxation has been associated theoretically with reduced band gap [15]. If the band gap were lower locally near the C atoms, PL might measure a lower band gap than the HBT transport measurement, in which carriers must move through the material. That the two techniques measured similar changes in band gap suggests that the band gap is spatially uniform.

3. Heterojunction internal photoemission structures

3.1. Device structure and principle

P^+-$Si_{1-x-y}Ge_xC_y$/p^--Si heterojunction internal photoemission (HIP) structures were fabricated. These consist of a heavily doped p^+-$Si_{1-x-y}Ge_xC_y$ layer on more lightly doped p-type Si. The large valance band offset ΔE_V between the Si and the $Si_{1-x-y}Ge_xC_y$ causes the current to be thermally activated in reverse bias ($V_{SiGeC} > V_{Si}$) so that the device rectifies at low temperature. The equilibrium valence band structure of this device is shown in Fig. 4.

3.2. Valence band offset measurement

In theory, ΔE_V in these structures may be measured by thermal activation of the leakage current. However, the leakage current for the entire device can easily be dominated by non-ideal sources at a few local defects. Therefore, to measure the band offset, we used capacitance techniques, which we found more reliable than leakage current measurements. The capacitance of the HIP structures was measured as a function of reverse bias at 100 K. Much like a Schottky barrier or a one-sided p–n junction, the capacitance per unit area C [16] is given by

$$\frac{1}{C^2}=\frac{2(\phi-V)}{q\epsilon N_A} \quad (3)$$

$$\phi=\Delta E_V - qE_f - kT/q - \Delta \quad (4)$$

where V is the d.c. bias, N_A is the dopant concentration on the Si side of the heterojunction, E_f is the position of the Fermi level relative to the valence band of the $Si_{1-x-y}Ge_xC_y$, and Δ is the image force barrier lowering. By extrapolating $1/C^2$ to zero, we extracted ϕ for devices with different Ge and C contents.

Assuming that only ΔE_V on the right-hand side of Eq. (4) is a function of C content, we converted the extracted ϕ values into ΔE_V and found that $\delta\phi/\delta y = \delta(\Delta E_V)/\delta y = -20$ meV %C^{-1}. The valence band offset is plotted as a function of C content in Fig. 5. The absolute magnitudes of ΔE_V were set to the values calculated for pseudomorphic $Si_{1-x}Ge_x$ [13], such that $\Delta E_V = 0.84x$ for $y=0$. Note that the slopes were nearly identical for both Ge contents and that the scatter

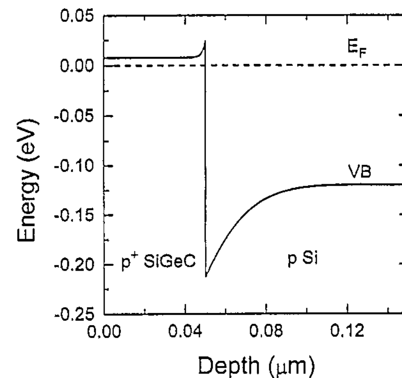

Fig. 4. Zero-bias valence band diagram of the heterojunction internal photoemission (HIP) structure.

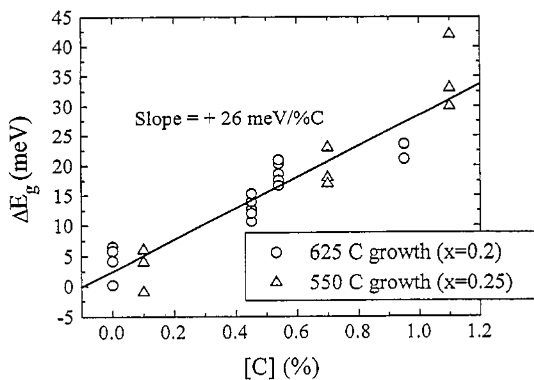

Fig. 3. ΔE_G measured by the HBT collector current as a function of C fraction for the 550 and 625 °C devices.

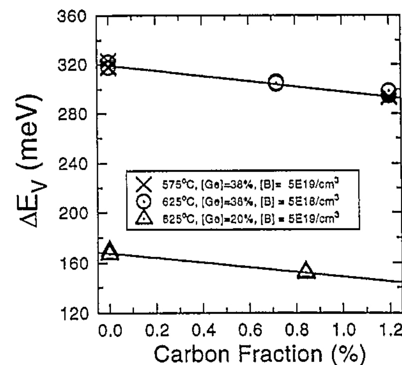

Fig. 5. $Si_{1-x-y}Ge_xC_y$ valence band offset to Si measured by the capacitance of the HIP structure as a function of C content.

in the data was minimal. For that reason we regard this measurement as more reliable than our previous measurement of ΔE_V by thermionic emission [17].

Recall that previously we showed that the band gap of $Si_{1-x-y}Ge_xC_y$ increases by 21–26 meV $\%C^{-1}$. Now we see that most of that (about 75%–95%) is due to movement of the valence band and a much smaller portion (less than 25%) is due to movement of the conduction band.

Previously reported measurements of $W/Si_{1-x-y}Ge_xC_y$ Schottky diodes [18] indicated that the Schottky barrier to p-type $Si_{1-x-y}Ge_xC_y$ Φ_{Bp} increased approximately 240 meV $\%C^{-1}$ for $y \leq 0.007$, and the barrier to n-type $Si_{1-x-y}Ge_xC_y$ Φ_{Bn} was independent of x and y. According to Schottky barrier theory, $\Delta E_G = \Delta \Phi_{Bp} + \Delta \Phi_{Bn}$. Clearly, these results are inconsistent with our optical and electrical measurements of ΔE_G and ΔE_V. It is possible for states at the metal–semiconductor interface to cause Schottky barrier results to be substantially different than the offsets measured in our structures.

4. $Si_{1-x-y}Ge_xC_y$ p–i–n diodes

4.1. Diode fabrication

$Si_{1-x-y}Ge_xC_y$ p–i–n diodes were fabricated and characterized. The diodes consisted of 560 Å nominally undoped $Si_{0.8}Ge_{0.2}C_y$ layers sandwiched between in situ doped n- and p-type Si (Fig. 6). The $Si_{1-x-y}Ge_xC_y$ layers were grown at 625 °C, and the methylsilane flow was varied from 0 to 0.2 standard cm^3 min^{-1}. The diodes were formed by a single-mesa, two-mask process. First, the mesas were plasma etched in SF_6, and then the Ti(300 Å)/Al(1200 Å) metallization was patterned by lift-off. The approximately 0.5 μm high mesas were 180×320 μm, while the top metal contact was only about a third as large to allow optical access from the top surface.

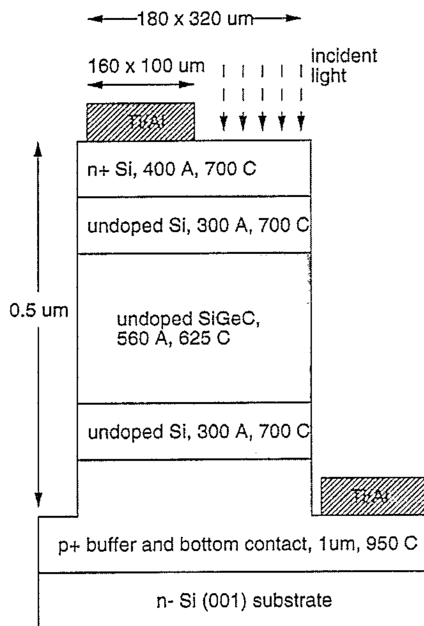

Fig. 6. Device structure of $Si_{0.8}Ge_{0.2}C_y$ p–i–n diodes. The p^+ layer was doped with 7×10^{18} cm^{-3} B, and the n^+ layer was doped with 3×10^{19} cm^{-3} P. The unintentionally doped region was found by spreading resistance to contain approximately 10^{17} cm^{-3} B.

4.2. Diode I–V characteristics

The current–voltage characteristics of several (about 10) randomly selected diodes from each wafer were measured. We compared the geometric mean of the *I–V* curves from each wafer. These curves are plotted in Fig. 7. There was no apparent forward-bias current trend with C concentration; the forward current ideality factor was approximately 1.8 for all concentrations, indicating that the forward current was due primarily to recombination in the depletion region. However, in reverse bias, the leakage current clearly increased and the breakdown voltage decreased with [C]. The C-free control sample and the 0.6% C sample displayed very similar *I–V* characteristics. The lack of increase in leakage may be an indication that at low C levels there is not a significant increase in recombination/generation centers. The diodes with the highest C content (1.2%) were clearly degraded compared with the control sample. The leakage at −3 V, for example, increased from 10^{-4} to 10^{-2} A cm^{-2}, and the breakdown became much softer and decreased from −9 V to approximately −5 V. Recall that the C concentrations were measured by XRD and that this method assumes that all C atoms are substitutional. The C fraction measured by this means has been shown to saturate at high methylsilane flow, whereas the true $[C_{total}]$ might not [19]. In that case, our sample with 1.2% C might contain a large amount of non-substitutional C, which would contribute electrically active generation/recombination centers [20].

At the intermediate C concentration (1.0%), the *I–V* behavior was bimodal: the diodes could be split into two groups with very different breakdown characteristics. About a third of the diodes had an *I–V* curve similar to those at lower [C] but with a somewhat higher leakage current and lower breakdown voltage. The other two-thirds had a significantly

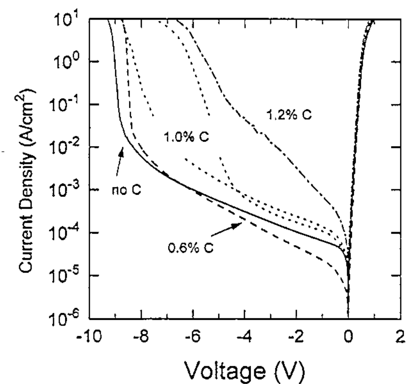

Fig. 7. $Si_{0.8}Ge_{0.2}C_y$ p–i–n diode current–voltage characteristics measured at room temperature.

lower breakdown voltage (approximately −6 V). If this lower breakdown voltage is caused by single, uncorrelated point defects, the yield of good devices Y [21] is given by

$$\ln Y = -A\delta \quad (5)$$

where A is the device area and δ is the defect density. Our case, with $Y=0.33$ and $A=5.8\times10^{-4}$ cm^2, yields a defect density δ of 1.9×10^3 cm^{-2} or an average defect spacing of 460 μm. this large defect spacing is difficult to understand if it is assumed that the defects are interstitial C or SiC precipitates. In both cases, one might expect a greater density of small defects.

4.3. Photoresponse

The reverse bias photocurrent of the $Si_{1-x-y}Ge_xC_y$ diodes was measured at room temperature. The photoresponse was due to photogeneration of electron–hole pairs by band-to-band absorption of the incident light. If all of the photogenerated electrons and holes are separated by the electric field and contribute current and if the absorbing layer is thin ($d\alpha \ll 1$), then the photocurrent is given by

$$I_{\text{photo}}(h\nu) = qd\alpha(h\nu)\frac{P(h\nu)}{h\nu} \quad (6)$$

where q is the electronic charge, d is the thickness of the absorbing layer, α is the absorption coefficient, P is the incident optical power, and $h\nu$ is the incident photon energy.

Band-to-band photon absorption in indirect band gap semiconductors such as Si and $Si_{1-x}Ge_x$ is primarily by means of phonon emission and absorption [22]. One expects an additional no-phonon process (as seen in photoluminescence) in $Si_{1-x}Ge_x$, but it has not yet been observed experimentally. The absorption coefficient is given by the Macfarlane–Roberts expression [23], which for photon energies between $E_G-\hbar\omega$ and $E_G+\hbar\omega$ is

$$\alpha(h\nu,T) = A\frac{(h\nu-E_G-\hbar\omega)^2}{1-\exp(-\hbar\omega/kT)} \quad (7)$$

where $\hbar\omega$ is the phonon energy; and for photon energies greater than $E_G+\hbar\omega$ the expression is

$$\alpha(h\nu,T) = A\left[\frac{(h\nu-E_G-\hbar\omega)^2}{1-\exp(-\hbar\omega/kT)}+\frac{(h\nu-E_G+\hbar\omega)^2}{\exp(\hbar\omega/kT)+1}\right] \quad (8)$$

The photoresponse is the photocurrent divided by the photon flux $P/h\nu$ and is proportional to the absorption coefficient. In Fig. 8 we have plotted the spectral photoresponse of three $Si_{1-x-y}Ge_xC_y$ devices and an all-Si control device (same structure but with an all-Si undoped region). At low energy ($h\nu<1.3$ eV), the $Si_{1-x-y}Ge_xC_y$ devices, owing to the small band gap material, exhibited a photoresponse larger than that of the all-Si device. Furthermore, these data exhibited a trend with C fraction agreeing with previous luminescence measurements [3,4]. As C was added to the $Si_{1-x}Ge_x$, the photoresponse decreased and shifted towards that of the all-Si device. This trend is consistent with the band gap increasing, and thus absorption decreasing, with the addition of C.

Extracting the band gap of indirect semiconductors from photoresponse (or absorption) data is done most reliably by plotting the square-root of the photoresponse as a function of photon energy [22]. Doing so for the all-Si device, we found as predicted by Eq. (7) and Eq. (8) that the square-root of the photoresponse was well fit by two straight-line segments. The segment corresponding to phonon absorption intersects the energy axis at $E_G-\hbar\omega$, and the other segment corresponding to phonon emission intersects the axis at $E_G+\hbar\omega$. Our fit gave $E_G=1.10$ eV and $\hbar\omega=70$ meV, close to the known values for Si of 1.12 eV and 58 meV respectively.

Fig. 9 shows the square-root of the photoresponse of three $Si_{1-x-y}Ge_xC_y$ diodes. These data cannot be fitted to two straight lines as was done for the all-Si device. While the region above 1.00 eV showed the expected quadratic behavior, the photoresponse did not go to zero at $E_G-\hbar\omega$ (approximately 0.90 eV), as predicted by Eq. (7). These diodes exhibited excess deep absorption, which increased with the C concentration. We can be reasonably certain that the origin of this excess absorption is electrically active defect states within the band gap, but we do not know whether the defects

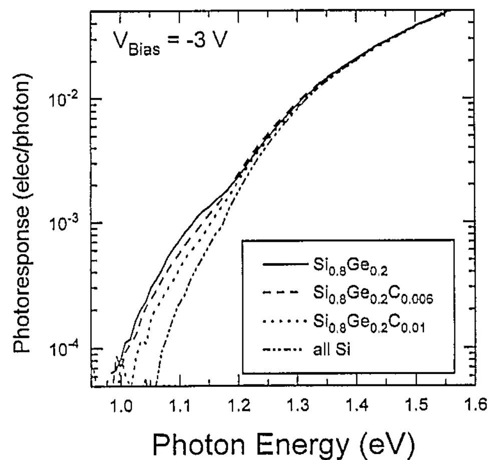

Fig. 8. $Si_{0.8}Ge_{0.2}C_y$ and all-Si p–i–n diode room temperature photoresponse.

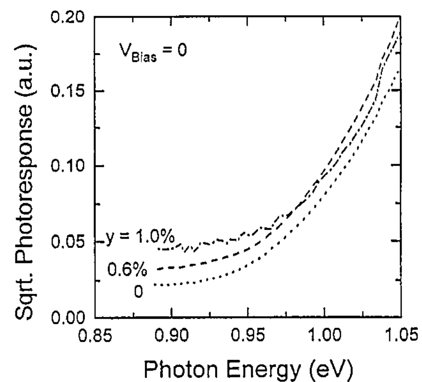

Fig. 9. Square-root of the room temperature photoresponse of the $Si_{0.8}Ge_{0.2}C_y$ diodes.

are due to substitutional C, interstitial C, or to impurities (such as O) in the methylsilane source gas, which might also increase as [C] increased. However, it must be noted that the C-free device showed this absorption tail as well, and at least four earlier independent photocurrent experiments on strained $Si_{1-x}Ge_x$ grown by low temperature epitaxy suffered similarly from sub-E_G defect absorption [24–27]. These observations suggest that although the deep absorption increased fourfold when the C content was raised from 0 to 1.0%, the defects responsible may not be due solely to the presence of C.

5. Summary

For a given band gap, pseudomorphic $Si_{1-x-y}Ge_xC_y$ thin films on Si (001) have less strain and presumably a greater critical thickness than do C-free $Si_{1-x}Ge_x$ films [4]. $Si_{1-x-y}Ge_xC_y$ layers with reduced strain may offer the possibility of extending Si-based heterostructures to applications requiring thicker films than are currently available with $Si_{1-x}Ge_x$.

We have fabricated and characterized three sets of microelectronic devices containing epitaxial $Si_{1-x-y}Ge_xC_y$ layers. The temperature dependence of the collector current in $Si_{1-x-y}Ge_xC_y$ base heterojunction bipolar transistors indicated that the band gap of $Si_{1-x-y}Ge_xC_y$ increases +26 meV $\%C^{-1}$ [7]. Capacitance measurements on p^+-$Si_{1-x-y}Ge_xC_y/p^-$-Si heterojunction internal photoemission structures indicated that the increase in band gap in the $Si_{1-x-y}Ge_xC_y$ is due primarily to downward movement of the valence band. Finally, $Si_{1-x-y}Ge_xC_y$ p–i–n diodes showed no degradation in reverse bias leakage compared with C-free devices for $y < 0.01$. However, the diodes did exhibit excess sub-band gap absorption which increased with [C].

Acknowledgements

We thank Helena Gleskova and Vladimir Bulović for assistance with the p–i–n diode photocurrent measurements. The support of ONR and USAF Rome Lab is gratefully acknowledged.

References

[1] K. Eberl, S. Iyer, S. Zollner, J. Tsang and F. LeGoues, *Appl. Phys. Lett., 60* (1992) 3033.
[2] J. Regolini, F. Gisbert, G. Dolino and P. Boucaud, *Mater. Lett., 18* (1993) 57.
[3] P. Boucaud, C. Francis, F. Julin, J. Lourtioz, D. Bouchier, S. Bodnar, B. Lambert and J. Regolini, *Appl. Phys. Lett., 64* (1994) 875.
[4] A.St. Amour, C. Liu, J. Sturm, Y. Lacroix and M. Thewalt, *Appl. Phys. Lett., 67* (1995) 3915.
[5] K. Brunner, K. Eberl and W. Winter, *Phys. Rev. Lett., 76* (1996) 303.
[6] J. Matthews and A. Blakeslee, *J. Cryst. Growth, 27* (1974) 118.
[7] L. Lanzerotti, A.St. Amour, C. Liu, J. Sturm, J. Watanabe and N. Theodore, *Electron Devices Lett.*, (1996) to be published.
[8] C. Liu, A.St. Amour, J. Sturm, Y. Lacroix, M. Thewalt, C. Magee and D. Eaglesham, *J. Appl. Phys.*, (1996) to be published.
[9] C. King, J. Hoyt and J. Gibbons, *IEEE Trans. Electron Devices, 36* (1989) 2093.
[10] H. Kroemer, *Proc. IEEE, 70* (1982) 12.
[11] E. Prinz, P. Garone, P. Schwartz, X. Xiao and J. Sturm, *IEEE Electron Devices Lett., 12* (1991) 42.
[12] J. Slotboom, G. Streutker, A. Pruijmboom and D. Gravesteijn, *IEEE Electron Devices Lett., 12* (1991) 486.
[13] C. Van de Walle and R. Martin, *Phys. Rev. B, 34* (1986) 5621.
[14] B. Dietrich, H. Osten, H. Rücker, M. Methfessel and P. Zaumseil, *Phys. Rev. B, 49* (1994) 49.
[15] A. Demkov and F. Sankey, *Phys. Rev. B, 48* (1993) 2207.
[16] S. Forrest and O. Kim, *J. Appl. Phys., 52* (1981) 5838.
[17] C. Chang, A.St. Amour, L. Lanzerotti and J. Sturm, *Mater. Res. Soc. Symp. Proc., 402* (1995) 437.
[18] M. Mamor, C. Guedj, P. Boucaud, F. Meyer and D. Bouchier, *Mater. Res. Soc. Symp. Proc., 379* (1995) 137.
[19] S. Bodnar and J. Regolini, *J. Vac. Sci. Technol. A, 13* (1995) 2336.
[20] G. Davies and R. Newman, *Handbook on Semiconductors,* Vol. 3b, Elsevier, New York, 1994, pp. 1558–1635.
[21] W. Runyan and K. Bean, in *Semiconductor Integrated Circuit Processing Technology*, Addison-Wesley, New York, 1990, Chapter 11.
[22] R. Braunstein, A. Moore and F. Herman, *Phys. Rev., 109* (1958) 695.
[23] G. Macfarlane and V. Roberts, *Phys. Rev., 97* (1955) 1714.
[24] D. Lang, R. People, J. Bean and A. Sergent, *Appl. Phys. Lett., 47* (1985) 1333.
[25] J. Park, R. Karunasiri and K. Wang, *J. Vac. Sci. Technol. B, 8* (1990) 217.
[26] A.A. Chowdhury, M.M. Rashed, C. Mazier, S. Murtaza and J. Cambell, *J. Vac. Sci. Technol. B, 11* (1993) 1685.
[27] S. Murtaza, R. Mayer, M. Rashed, D. Kinosky, C. Mazier, S. Banerjee, A. Tasch, J.C. Campbell, J.C. Bean and L.J. Peticolas, *IEEE Trans. Electron Devices, 41* (1994) 2297.